NEOPLASIA
www.neoplasia.com
Volume 23 Number 8 August 2021 pp. 823–834

Original research

miR-138-5p induces aggressive traits by targeting *Trp53* expression in murine melanoma cells, and correlates with poor prognosis of melanoma patients ☆, ☆☆

Adriana Taveira da Cruz [a]; Aline Hunger [b,c]; Fabiana Henriques Machado de Melo [a,d]; Ana Carolina Monteiro [a,e]; Geneviève Catherine Paré [f]; Dulce Lai [f]; Débora Kristina Alves-Fernandes [a]; Ana Luisa Pedroso Ayub [a]; Esteban Mauricio Cordero [g]; José Franco da Silveira Filho [g]; Regine Schneider-Stock [e]; Bryan Eric Strauss [b]; Victor Tron [f,g]; Miriam Galvonas Jasiulionis [a,*]

[a] Department of Pharmacology, Escola Paulista de Medicina, Universidade Federal de São Paulo, São Paulo, SP, Brazil
[b] Laboratório de Vetores Virais, Centro de Investigação Translacional em Oncologia/LIM24, Instituto do Câncer do Estado de São Paulo, Faculdade de Medicina, Universidade de São Paulo, SP, Brazil
[c] Current address: Cristalia, Biotecnologia Unidade 1, Rodoviária SP 147, Itapira, SP, Brasil
[d] Department of Pharmacology, Institute of Biomedical Science, University of São Paulo, São Paulo, SP, Brazil
[e] Department of Pathology, Friedrich-Alexander Universität, Erlangen, Bavaria, Germany
[f] Department of Pathology and Molecular Medicine, Queen's University, Kingston, Ontario, Canada
[g] Microbiology, Immunology and Parasitology Department, Universidade Federal de São Paulo, São Paulo, SP, Brazil

Abstract

Deregulation of miRNAs contributes to the development of distinct cancer types, including melanoma, an aggressive form of skin cancer characterized by high metastatic potential and poor prognosis. The expression of a set of 580 miRNAs was investigated in a model of murine melanoma progression, comprising non-metastatic (4C11-) and metastatic melanoma (4C11+) cells. A significant increase in miR-138-5p expression was found in the metastatic 4C11+ melanoma cells compared to 4C11-, which prompted us to investigate its role in melanoma aggressiveness. Functional assays, including *anoikis* resistance, colony formation, collective migration, serum-deprived growth capacity, as well as *in vivo* tumor growth and experimental metastasis were performed in 4C11- cells stably overexpressing miR-138-5p. miR-138-5p induced an aggressive phenotype in mouse melanoma cell lines leading to increased proliferation, migration and cell viability under stress conditions. Moreover, by overexpressing miR-138-5p, low-growing and non-metastatic 4C11- cells became highly proliferative and metastatic *in vivo*, similar to the metastatic 4C11+ cells. Luciferase reporter analysis identified the tumor suppressor *Trp53* as a direct target of miR-138-5p. Using data sets from independent melanoma cohorts, miR-138-5p and P53 expression were also found deregulated in human melanoma samples, with their levels negatively and positively

* Corresponding author.
E-mail address: mjasiulionis@gmail.com (M.G. Jasiulionis).
☆ Funding: This work was financially supported by grants from Fundação de Amparo à Pesquisa do Estado de São Paulo (2010/18484-6, 2012/08776-5, 2014/13663-0, and 2018/20775-0), Coordenação de Aperfeiçoamento de Pessoal de Nível Superior (2867/10), and Conselho Nacional de Desenvolvimento Científico e Tecnológico (473139/2009-0). AM was a common Cotutelle PhD student of Universidade Federal de São Paulo and the University Hospital of Friedrich Alexander University Erlangen under supervision of MJ and RSS.
☆☆ Conflict of interest: The authors declare that they have no known competing financial interests or personal relationships that could have appeared to influence the work reported in this paper. The authors declare that they have no competing interests.
Received 19 February 2021; received in revised form 10 May 2021; accepted 31 May 2021

https://doi.org/10.1016/j.neo.2021.05.015

correlated with prognosis, respectively. Our data shows that the overexpression of miR-138-5p contributes to melanoma metastasis through the direct suppression of *Trp53*.

Neoplasia (2021) 23, 823–834

Keywords: Melanoma, miR-138-5p, *Trp53*, Metastasis, Aggressiveness

Background

Cutaneous malignant melanoma is the most aggressive type of skin cancer. It arises from the malignant transformation of melanocytes, and accounts for about 75% of skin cancer-related deaths, what is associated with its high metastatic capability. Alterations in specific signaling pathways play a central role in melanoma development and progression. Components of the RAS/RAF/MEK/ERK pathways are frequently mutated in melanoma and favor tumor growth and apoptosis evasion [43]. However, in addition to NRAS and BRAF other pathway components are frequently altered in human melanoma cell lines and melanoma samples, such as CDKN2A/CDK4, PI3K/AKT, WNT/β-catenin, NOTCH and P53 [28]. Yu and colleagues [55] demonstrated that the disruption of p53 in a subpopulation of primary human melanocytes with altered expression of BRAF leads to rapid cell growth, suggesting a role of p53 alterations in melanocyte malignant transformation. In fact, p53 has been shown to suppress the progression from benign nevi to melanoma [36]. According to The Cancer Genome Atlas (TCGA) consortium approximately 17% of melanomas harbor *TP53* mutations [13]. Even though wild-type p53 expression is found in over 80% of melanomas, it is frequently inactivated. Therefore, other mechanisms must be associated with abnormal p53 activity, such as increased MDM2 activity and abnormal regulation by miRNAs [10,18,34,35,41].

MicroRNAs (miRNA) are short non-coding RNAs that regulate mRNA expression of target genes leading to mRNA degradation or translational repression. In cancer development, miRNAs regulate many processes, such as proliferation, apoptosis, angiogenesis and metastasis [44] and are, therefore, promising targets to be used in cancer treatment. Several microRNAs were described as differentially expressed between melanocytes and melanomas as well as in melanoma cell lines, being classified as oncogenes or tumor suppressors, and associated with poor outcomes [5,12]. Global miRNA expression studies showed evidence that miRNAs, including miR-138-5p, are deregulated during melanoma progression [11,17,29]. This miRNA has been used as therapy in distinct types of cancer such as chronic myeloid leukemia and non-small-cell lung cancer [42]. However, high expression of miR-138 was associated with poor survival in glioma [6].

In the present work, we investigated the role of miR-138-5p in melanoma progression. This miRNA was selected after the evaluation of global expression of miRNAs in a linear model of murine melanoma progression established in our laboratory. The model consists of different cell lines representing normal melanocytes (melan-a), pre-malignant melanocytes (4C), non-metastatic melanoma (4C11-) and metastatic melanoma (4C11+) cells [27,32,45]. Here, we show that mmu-miR-138-5p promotes an aggressive melanoma phenotype through modulation of p53 expression. Additionally, by analyzing independent human melanoma data sets, we have found that high hsa-mir-138-5p expression and low P53 expression correlate with poor outcome in melanoma patients.

Methods

Cell culture

The murine non-tumorigenic melanocyte lineage melan-a [4] was cultured in a 37°C incubator with 95% humidified air and 5% CO_2. Cells were maintained in RPMI pH 6.9, supplemented with 5% (v/v) fetal bovine serum (Invitrogen, Scotland, UK), 200 nM phorbol 12-myristate 13-acetate (PMA; Calbiochem, Darmstadt, Germany), 100 U/mL penicillin, and 100 µg/mL streptomycin (Invitrogen, Grand Island, NY, USA). Murine pre-malignant melanocytes 4C, non-metastatic melanoma cells 4C11−, metastatic melanoma cells 4C11+, as well as the cells overexpressing mmu-miR-138-5p, named 4C11- miR-138, and the 4C11- mock control, were cultured as melan-a cells, but in the absence of PMA.

MicroRNA analysis by NanoString technology

Total RNA, including miRNAs, from 4C11- and 4C11+ melanoma cells was prepared in triplicate using the miRNeasy Mini kit (Qiagen, Hilden, Germany). DNA digestion was performed according to the manufacturer's protocol. A total of 580 miRNAs were profiled in 4C11- and 4C11 + cells by the nCounter Mouse v1.5 miRNA Assay (NanoString Technologies, Seattle, WA, USA). As recommended by the manufacturer, 100 ng of total RNA was used as input for sample preparation. RNA and specific probes were hybridized overnight at 65°C, automatically processed in the Prep Station and transferred to the Digital Analyzer for data collection. The NanoString nSolver software was used for normalization and pair-wise comparisons. miRNA data was normalized with the 100 most highly expressed miRNAs. Based on background detection the minimal threshold for detection of a miRNA was considered as 50 counts.

Retrovirus production, infection, and establishment of stable 4C11- cell line overexpressing miR-138-5p

Murine miR-138-5p precursor coding sequence is located in two different chromosomes, with pre-miR-138/1 transcribed from chromosome 9 and pre-miR-138/2 from chromosome 8. Given that the mature sequence derived from both precursors is identical, the copy encoded by chromosome 8 was chosen to generate the construct. Coding sequence of pre-miR138/2, including its flanking regions, were amplified by PCR using the following primers: F: 5'GGTA**GAATTC**GGGTTCTGGGCTTTCTACCTTC3' and R: 5' GGTA**GGATCC**CTTCCCAGGTGACTATGAGGTG3'. Amplicons were digested with EcoRI and BamHI restriction endonucleases (restriction sites are highlighted in the primers sequences) and ligated into the same restriction sites of pCLXSN retrovirus expression vector [33]. After the virus production, the non-metastatic 4C11- cells were transduced with a multiplicity of infection (MOI) of 1 and selected for neomycin resistance (1 mg/mL) to generate the stable 4C11- miR-138 cell line, overexpressing mmu-miR-138-5p and 4C11- mock, harboring the empty vector.

mRNA RT-PCR

RNA was isolated from samples using Trizol (Invitrogen, Carlsbad, CA) according to the manufacturer's specification. Equal amounts of each cDNA synthetized were quantified by real-time PCR in a Corbett Rotor-Gene 6,000 Detection System version 1.7 using a SYBR green PCR master mix (Qiagen, Dusseldorf, German). The relative expression of *Trp53* was determined using the following primers: *Trp53* forward 5' CAAGAAGGGCCAGTCTACTTCC 3', *Trp53* reverse 5' ACTCCAACAGACTGCCTGGA 3', *Actin* forward 5' CGAGGCCCAGAGCAAGAGAG 3'; *Actin* reverse 5' AGGAAGAGGATGCGGCAGTGG 3'. Relative quantification (RQ) of the amplicons was calculated according to the 2-ΔΔCq method. β-actin was used as an endogenous expression control.

Indirect immunofluorescence

For P53 staining, cell lines were grown as a monolayer on 10 mm-round glass coverslips and fixed in 3.7% paraformaldehyde. For phospho-FAK and phalloidin staining, cells were grown as a monolayer on 10 mm-round glass coverslips to 100% confluence followed by the generation of a wound using a pipette tip. After 15 min, cells were fixed in 3.7% paraformaldehyde. Coverslips were blocked with 1% BSA-PBS for 30 min at room temperature. Cells were incubated for 1 h with mouse anti-P53 antibody (Sigma-Aldrich #P5813) or anti-pFAK (Millipore) at room temperature, washed 3 times with 1% BSA-PBS, and incubated with an Alexa 488–conjugated anti-mouse IgG antibody (Molecular Probes, Carlsbad, CA) for 45 min and for 5 min with 4',6-diamidino-2-phenylindole (DAPI). Phalloidin-rhodamine was incubated for 30 min. After washing in PBS, slides were mounted with antifade solution and analyzed in a fluorescence microscope (Carl Zeiss, Göttingen, Germany).

MicroRNA real-time PCR

Total RNA from cell lines was isolated using the miRNeasy mini kit (Qiagen) according to the manufacturer's protocol. mmu-miR-138-5p or hsa-miR-138-5p level was determined using a TaqMan miRNA assay (Applied Biosystems, Foster City, CA) according to the manufacturer's protocol. miRNA expression was assayed in triplicate, and data were normalized to endogenous RNU6B. The relative level was calculated using the ΔΔCT method.

Western blotting

Protein extracts were prepared using lysis buffer (1% Triton X−100 in 150 mM NaCl and 50 mM Tris at pH 7.4, containing 5 mM EDTA, 2 µg/mL aprotinin, 1 mM PMSF and 1 mM $NaVO_4$), kept on ice for 15 min, followed by centrifugation at 10,000 rpm for 15 min at 4°C. The supernatant was collected and protein concentration was measured using the Bio-Rad Protein Assay Dye Reagent (Bio-Rad, Hercules, CA). Equivalent amounts of protein (50 μg) were denatured in SDS sample buffer (240 mM Tris–HCl at pH 6.8, 0.8% SDS, 200 mM b-mercaptoethanol, 40% glycerol and 0.02% bromophenol blue) for 5 min at 100°C, then separated by electrophoresis on SDS-PAGE and transferred to a polyvinylidene difluoride membrane (Amersham, Piscataway, NJ). After protein transfer, the membranes were blocked using 5% nonfat dry milk in TBS (10 mM Tris-HCl pH 7.2, 150 mM NaCl) and incubated with a primary antibody overnight at 4°C, followed by incubation with the appropriate HRP-conjugated secondary antibody and subsequent development using a chemiluminescent substrate (SuperSignal West Pico Chemiluminescent Substrate; Pierce Chemical, Rockford, IL). The antibodies utilized were: anti-γ-tubulin (Sigma-Aldrich #T6557), anti-P53 (Sigma-Aldrich #P5813), and anti-β-actin (Santa Cruz Biotechnology #1616). To assess whether MDM2 was responsible for the downregulation of P53 protein, melan-a and 4C11+ cells were cultured during 24 h followed by a 6 h treatment with 20 µM of the proteasome inhibitor MG-132 (Sigma-Aldrich, Missouri, USA) or DMSO (Sigma-Aldrich, Missouri, USA) for negative control. After treatment, cells were harvested by mild-trypsin treatment and total protein was extracted and analyzed by Western blotting as previously described.

Vector construction and luciferase reporter assay

Vector construction and luciferase activity analyses were performed as described [8]. The construct pGL3-*Trp53* 3'UTR was generated by amplifying a 544 bp 3′-UTR fragment from the murine *Trp53* gene covering the mmu-miR-138-5p binding site, which was predicted by the *TargetScan* server [1]. The primer sequences used for amplification were: F: 5'-GGTA**TCTAGA**CAATGGTCAAGAAAGTGGGGCC-3' and R: 5'-GGTA**TCTAGA**CCTCCCAAATTCATCCTGCCC-3' (XbaI restriction site are highlighted). The amplicons were purified and cloned into the pGL3-control vector (Promega, Madison, WI) at the *Xba* I site immediately downstream from the firefly luciferase.

The 4C11-, 4C11- mock, 4C11- miR-138 and 4C11+ cells were seeded on 12-well plates (75,000 cells per well) 1 d before the transfection and then cotransfected with pGL3-p53 3'UTR or pGL3 empty vector and *Renilla* luciferase vector (pRL-TK). Luciferase activity was measured 48 h after transfection using the Dual-Glo Luciferase Assay System (Promega). The *Renilla* luciferase activity served as internal control for signal normalization.

Proliferation and anoikis *resistance*

To evaluate the number of *anoikis*-resistant cells, a resazurin-based assay was performed. Adherent 4C11-, 4C11- mock, 4C11- miR-138 and 4C11+ cells were harvested by mild-trypsin treatment and 1×10^5 cells were cultured on 100 mm-diameter plates coated with agarose 1% (w/v). After 96 h under suspension condition, cells were collected, transferred to 96-well plates, and incubated with Alamar Blue (Invitrogen, California, USA) for two hours. The fluorescence emission was measured at a wavelength of 590 nm with an excitation of 560 nm using the SpectraMax M2 spectrofluorometer (Molecular Devices, California, USA). To assess proliferation capacity, 4C11-, 4C11- mock, 4C11- miR-138 and 4C11+ cell lines were plated in 96-well plates (3.5×10^3 cells/well). After 24, 48, 72 and 96 h, Alamar Blue was added and cells were incubated for 2 h. The fluorescence was measured as described above. Both experiments were performed in triplicate.

Wound healing assay

The collective migratory capability of 4C11-, 4C11- mock, 4C11- miR-138 and 4C11+ cell lines was estimated by wound healing assay. Cells were grown on 10 mm-round glass coverslips to 100% confluence followed by the generation of a wound using a pipette tip. Cells were then washed with PBS for removal of debris and maintained in culture for 24 h in serum-free medium. The distances between the edges were analyzed at time zero and after 24 h and the images were captured using the Photoshop CS Extended software (California, USA). Alternatively, the actin cytoskeleton and focal adhesion formation were analyzed in cells on the region of scratch by immunofluorescence.

Colony formation assay

4C11-, 4C11- miR-138 and 4C11+ cell lines were harvested and 200 cells were seeded into 60 mm-diameter plates to evaluate colony formation capability. After 10 days, the colonies formed were washed with PBS, fixed with 3.7% paraformaldehyde for 15 min, stained with 1% Toluidine Blue

for 5 min, washed with water and photographed. For quantification of viable cells, the dye was lysed, the dye solubilized in 1% SDS for 4 h and the absorbance at 620 nm was measured.

Tumorigenesis assay

4C11-, 4C11- mock, 4C11- miR-138 and 4C11+ cell lines were injected subcutaneously (s.c.) in the flank of 8-wk-old syngeneic C57Bl/6 female mice (2.5×10^5 cells per animal). After 10 d of inoculation, tumor sizes were measured daily and tumor volume calculated as: d^2 x D/2, where d corresponds to the smallest tumor diameter and D to the largest one. Each experimental group comprised at least five animals. All animal procedures used in this study were approved by the Ethics Committee from Universidade Federal de São Paulo (number 2118/11). This experiment was performed twice (n = 5 per group).

In vivo *lung colonization*

2.5×10^5 cells of 4C11-, 4C11- mock, 4C11- miR-138 and 4C11+ cell lines were injected into the lateral tail vein of 8-wk-old syngeneic C57Bl/6 mice with a 27-gauge needle. The mice were sacrificed 28 d after injection, lungs were surgically removed and metastatic foci were macroscopically scored. Each experimental group consisted of five animals. This experiment was performed in duplicate.

miR-138 antagomiR in vivo *tumorigenesis and lung colonization*

Ten nM of the miR-138 antagomiR (AM11727 Life Technologies, California, EUA) or 10 nM of the negative control (AM17010 Life Technologies, California, USA) were transfected in 4C11- miR-138 cell line according to the manufacturer's protocol. After 24-h incubation, 2.5×10^5 transfected-cells were injected in the mouse caudal vein or in the flank of C57Bl/6 mice as described previously. This experiment was performed twice.

Independent melanoma cohorts

For miR-138 expression analyses, total RNA from 26 formalin-fixed paraffin embedded (FFPE) tissue samples were isolated using RNA total Recovery All kit (Ambion, Texas, USA) following the manufacturer's instructions. The samples included 7 melanocytic nevi, 12 primary melanomas and 7 metastatic melanomas obtained from the Department of Pathology and Molecular Medicine from Kingston General Hospital, Kingston, Ontario, Canada. The study was approved by the Ethics Committee from Health Sciences College at Queen's University. miRNA level was determined using the TaqMan MicroRNA Assays (Applied Biosystems, Foster City, CA) according to the manufacturer's protocol. Hsa-miR-138-5p were assayed in triplicate and data were normalized to endogenous RNU6B. The relative levels were calculated using the ΔΔCt method.

Three melanoma data sets were accessed using the Melanoma Explorer tool (http://shiny.maths.usyd.edu.au/melanomaExplorer/), being one from TCGA (miRNA) [48], one from the New York University Set 1 cohort (miRNA), and another from the Sweden cohort (mRNA) [46]. For survival analyses, samples with mRNA or miRNA expression values below the lower threshold (25%) were taken to be in one group, whereas samples above the upper threshold (75%) formed the second group. Survival of patients in these two groups over time was visualized with a Kaplan-Meier plot and the significance of survival profile differences was computed using the log-rank test. Values above and below the median of hsa-mir-138 expression were considered for correlation analysis between tumor thickness and miRNA expression. Another melanoma data set extracted from the GSE8401 study was accessed using the Oncomine tool [39]. Melanoma protein data from TCGA was accessed using TCPA [19,20]. Details of each cohort, number of samples, methodologies, references and tools are available in the **Table S1**.

Statistical analysis

Data were analyzed using ANOVA or Student's t-test and Pearson correlation in SPSS 17.0 (SPSS Inc., Chicago, IL). $P \leq 0.05$ was considered statistically significant.

Results

miR-138-5p is highly expressed in metastatic melanoma cells

It is well known that numerous miRNAs are aberrantly expressed in different cancers, controlling the expression of oncogenes and tumor suppressor genes. In order to identify miRNAs that can be used as potential biomarkers for melanoma prognosis and diagnosis, we evaluated the expression of a set of 580 microRNAs in metastatic 4C11+ and non-metastatic 4C11-. We identified 25 miRNAs upregulated and 20 downregulated by at least 2.5-fold change in 4C11+ compared to the 4C11- cell line (**Tables S2** and **S3**, respectively). Among the 10-most upregulated miRNAs (**Figure 1A**), miR-138-5p was selected for further investigation. miR-138-5p expression was confirmed by quantitative stem-loop real-time reverse-transcription PCR. We observed that the metastatic melanoma cell line 4C11+ expresses high levels of miR-138-5p when compared to melan-a melanocytes, 4C pre-malignant melanocytes and the 4C11- non-metastatic melanoma cell line (**Figure 1B**). It is well established that miRNAs can promote tumorigenesis by altering the cell transcriptome, favoring growth, survival, and migration among other cancer-associated phenotypes. Thus, in this study we hypothesized that the alteration of miR-138-5p expression could contribute to melanoma progression, specifically through the gain of metastatic capabilities.

miR-138-5p overexpression confers aggressive traits to the non-metastatic melanoma cells

To evaluate the participation of miR-138-5p in melanoma progression, 4C11- cells, which express low endogenous level of the miRNA and are incapable of promoting metastasis, were transfected to stably overexpress the miR-138-5p. The stable expression levels of mature miR-138-5p in this cell line was evaluated by quantitative stem-loop real-time reverse-transcription PCR, which showed an increase of over 70-fold (**Figure 1D**). Following miR-138-5p overexpression in 4C11-, a clear change in cell morphology was observed. While 4C11- mock remained very similar to 4C11-, the morphology of 4C11- miR-138 was similar to the metastatic 4C11+ cells (**Figure 2A**). Differences in viability were also noted between the cell lines when maintained in FBS-free medium for 48h. The 4C11- miR-138 and 4C11+ were less susceptible to the absence of FBS in the culture medium compared to 4C11- and 4C11- mock (**Figure 2B**). Next, anchorage-independent growth and the capacity to overcome *anoikis* were measured. We observed that the 4C11- miR-138 cell line exhibits the greatest resistance to *anoikis* compared to all other cell lines, including the metastatic 4C11+ cell line (**Figure 2C**). Cell proliferation was also assessed with 4C11- miR-138 proliferating at a rate comparable to that of metastatic 4C11+ cell line, both of which proliferate much faster than the 4C11- mock cells (**Figure 2D**). Similar results were observed by colony formation, where 4C11- miR-138 formed colonies larger than 4C11-, and comparable to those generated by metastatic 4C11+ (**Figure 2E**).

Since metastatic 4C11+ cells express high levels of miR-138-5p, we hypothesize that this miRNA may contribute to the metastatic capacity of melanoma cells. In a wound healing assay, 4C11- miR-138 and 4C11+ cell

A

MicroRNAs upregulated in 4C11+ cells in comparison to 4C11- cells

miRNA name	4C11- counts	4C11+ counts	Fold change*
mmu-mir-211-5p	1	2417.88	2417.88
mmu-mir-10b-5p	1	505.54	505.54
mmu-mir-340-5p	1	172.83	172.83
mmu-mir-146a-5p	11.43	958.98	83.92
mmu-mir-34a-5p	3.18	105.67	33.22
mmu-mir-138-5p	4.15	119.82	**28.90**
mmu-mir-1198-5p	4.39	114.97	26.21
mmu-mir-129-3p	14.57	291.15	19.98
mmu-mir-126a-3p	22.96	335.69	14.62
mmu-mir-129-5p	7.55	64.41	8.54

* fold change ≥2.5

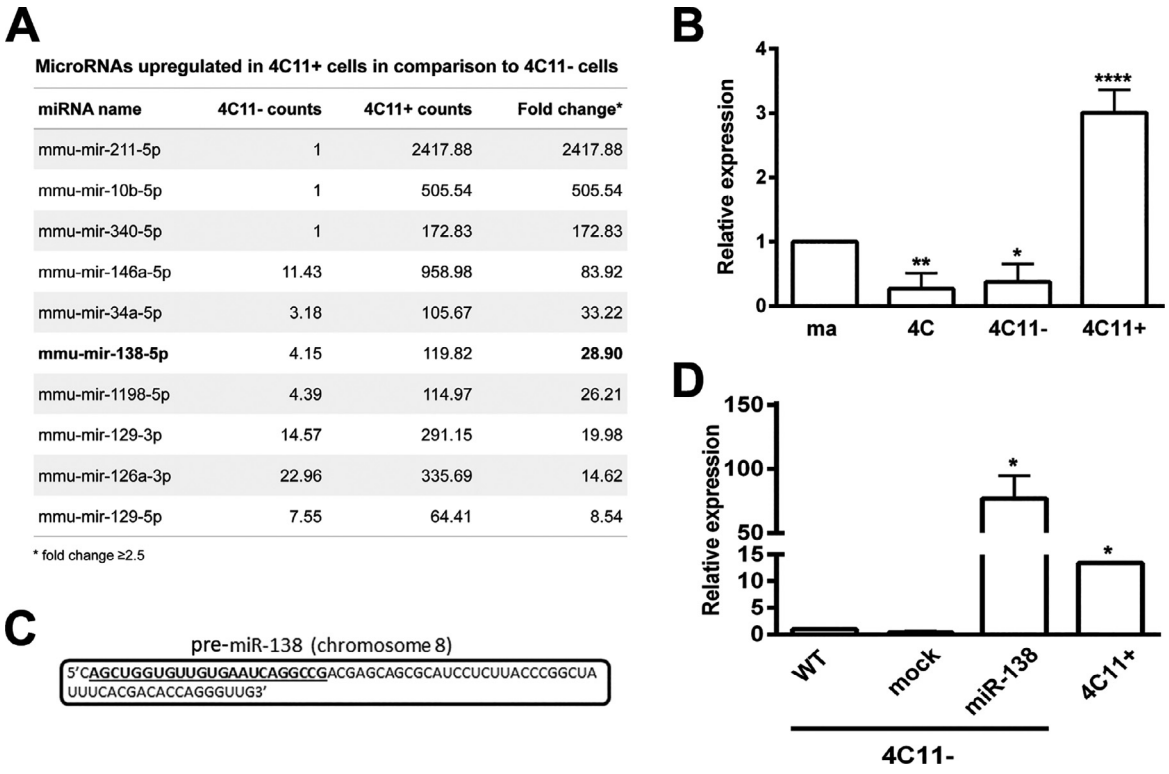

Fig. 1. miR-138-5p is highly expressed in metastatic cells, but not in the cell lines representing early stages of melanoma progression. **A.** Table showing the top 10 most upregulated miRNAs in metastatic 4C11+ compared to non-metastatic 4C11- cell line (FC >2.5), as evaluated by nCounter Mouse v1.5 miRNA Assay (NanoString Technologies). **B.** The expression of miR138-5p in cell lines representing different stages of melanoma progression, melan-a melanocytes (ma), pre-malignant melanocytes (4C), non-metastatic melanoma (4C11-) and metastatic melanoma cells (4C11+), was determined by real-time PCR. Mean +SEM; ANOVA $P < 0.0001$; Tukey post-test: * $P < 0.01$, ** $P < 0.001$, **** $P < 0.00001$. **C.** Pre-miR-138-5p/2 sequence and its chromosome of origin. **D.** The expression of mature miR-138-5p was determined by real-time PCR in melanoma cell lines transduced with the retroviral vector containing the pre-miR-138/2 sequence. U6 expression was used as endogenous control for miR-138-5p expression. Mean +SEM; ANOVA: $P = 0.0019$; Tukey post-test: * $P <$ 0.01. 4C11-: non-metastatic melanoma cell line; 4C11- mock: 4C11- transduced with viruses containing empty vector; 4C11- miR-138: 4C11- transduced with viruses encoding pre-miR138-5p and flanking region, and 4C11+: metastatic melanoma cell line.

lines exhibited greater collective migration rates compared to the tumorigenic 4C11- and 4C11- mock cell lines (**Figure 2**F). By immunofluorescence assay, we observed a reorganization of the actin cytoskeleton and membrane ruffling with the formation of p-FAK-positive lamellipodia in the leading edge of migratory 4C11- miR-138 and 4C11+, but not in 4C11- mock cells (**Figure S1**), reinforcing the migratory phenotype associated with the miR-138 expression.

4C11- cells overexpressing miR-138-5p develop fast-growing tumors and lung metastatic foci in vivo

Next, tumorigenesis and metastatic capacity of 4C11-, 4C11- mock, 4C11- miR-138 and 4C11+ cell lines were explored. To assess tumorigenesis, cells were injected s.c. into the flank of C57Bl/6 mice. Tumor volume was measured every two d starting from the 10th d post-injection until the 20th d, when mice were euthanized. While the tumors took an average of 10 d to develop in mice injected with 4C11- miR-138 and 4C11+ cells, no palpable tumors were detected in mice injected with 4C11- and 4C11- mock cells during the course of the assay (**Figure 3, A** and **B**). As previously shown, mice injected s.c. with 4C11- cells (2.5×10^5) took approximately 40 d prior to the development of tumors [45]. To assess the metastatic capacity of those cells, mice were injected with 2.5×10^5 cells via the caudal vein. After 28 d, animals were euthanized and the presence of metastatic foci in the lungs was evaluated. Equally to the metastatic cells 4C11+, all mice injected with 4C11- miR-138 cells presented numerous metastatic foci in the lungs. Moreover, number and size of foci were comparable (**Figure 3C**). No lung foci were detected in mice injected with 4C11- or 4C11- mock cell lines even after a prolonged period (*i.e.,* 60 d, data not shown).

miR-138-5p inhibition reverts the highly tumorigenic and metastatic capacity conferred by miR-138 overexpression

To confirm that overexpression of miR-138-5p is directly responsible for 4C11- miR-138 aggressive phenotype, these cells were transfected with an antagonist of miR-138-5p (anti-miR-138-5p) or a negative control. Twenty-four hours after anti-miR-138-5p transfection, miR-138-5p expression was significantly reduced in 4C11- miR-138 cells when compared to the negative control (**Figure 3D**). Cells treated with anti-miR-138-5p or anti-miR negative control were injected s.c. in the flank of C57Bl/6 mice. Palpable tumors were first detected on the 11th d post-injection in both groups. In average, tumor volume of mice injected with 4C11- miR-138 transfected with anti-miR-138-5p was about 1.5-fold smaller than those of the control group at the evaluated time points (**Figure 3E**). Additionally, metastatic capability was assessed by the *in vivo* lung colonization assay which revealed a significant reduction of metastatic foci in the mice injected with 4C11- miR-138 transfected with the anti-miR-138-5p compared to those injected with the negative control (**Figure 3F**). While the last group exhibited lungs

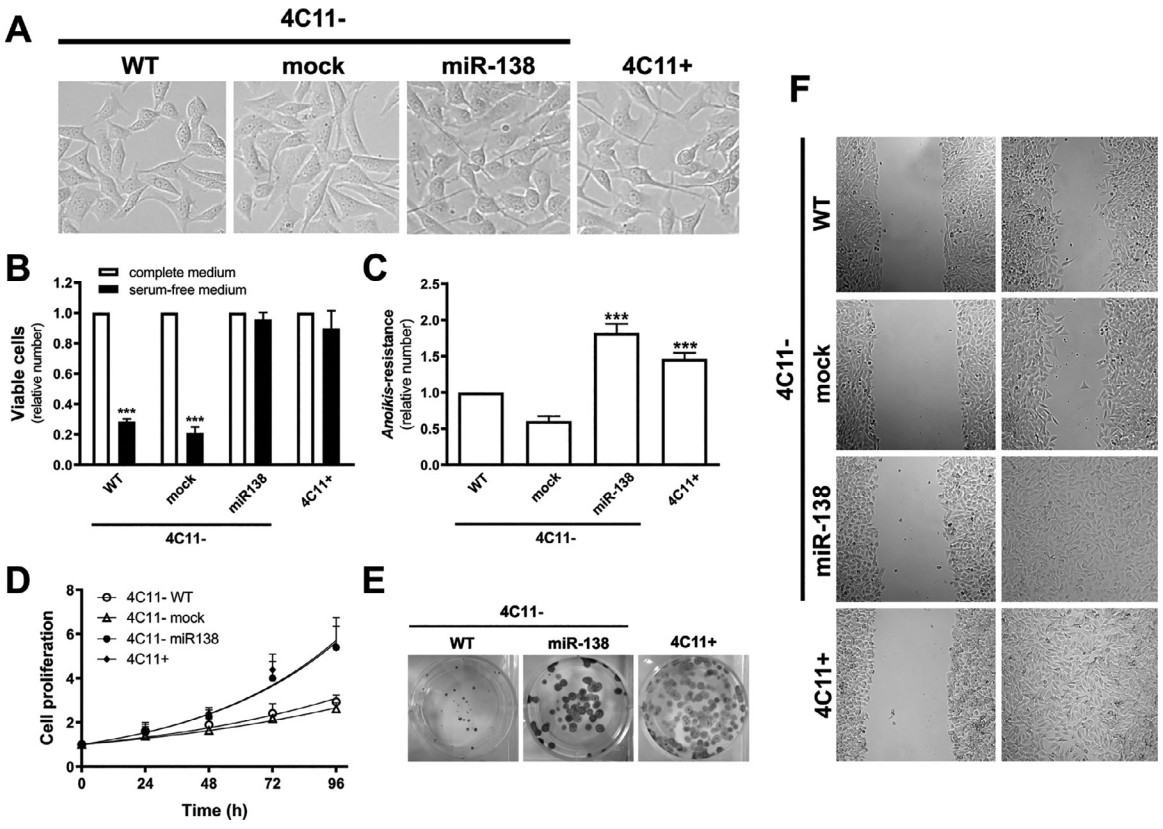

Fig. 2. miR-138-5p overexpression in non-metastatic melanoma cells increased proliferation, resistance to *anoikis,* growth under stress, colony formation, and collective migration. **A.** Photomicrographs showing morphological aspects of the non-metastatic 4C11- cells, its derived cell lines 4C11- mock and miR-138, and the metastatic 4C11+. **B.** Relative number of viable cells after culture for 48 h in RPMI medium with or without FBS. Mean+SEM; ANOVA and Tukey post-test: *** $P < 0.0001$. **C.** *Anoikis*-resistant cells after culture in suspension for 96 h. Mean+SEM; Anova $P < 0.0001$; Tukey post-test: *** $P < 0.0001$. **D.** Exponential growth curve where cell viability was measured with MTT at the indicated time points. **E.** Colony formation after culturing the cells for 10 d. **F.** Collective cell migration assessed using a wound healing assay evaluated 24 h after introduction of the scratch. 4C11- WT: non-metastatic melanoma cell line; 4C11- mock: 4C11- transduced with viruses containing empty vector; 4C11- miR-138: 4C11- transduced with virus containing the pre-miR138-5p and flanking sequences, and 4C11+: metastatic melanoma cell line.

completely taken by metastatic foci, the first presented few and isolated foci, clearly demonstrating the involvement of miR-138-5p in metastasis.

Trp53 *is a direct target of miR-138-5p in melanoma cells*

An *in-silico* analysis to search putative targets of miR-138-5p was performed on five different softwares (TargetScan 6.2 version, miRanda-mirSVR, MicroCosm Target, Diana Tools, and miRWalk). All algorithms identified *Trp53* as a potential target of miR-138-5p. Although it has been previously shown that miR-138 directly targets the 3' untranslated region (UTR) of *Trp53* and decreases its expression in different cells, such as in induced pluripotent stem cells [54] and macrophages [51], the regulation of p53 expression by direct binding of miR-138-5p in tumor cells has not yet been shown.

Then, we first explored the possible correlation between miR-138-5p and p53 protein expression in our murine model of melanoma progression. Interestingly, in all cell lines that encompass the cellular mouse model of melanoma genesis, p53 mRNA and protein are inversely correlated to miR-138-5p expression, suggesting that *p53* could be a direct target of this miRNA. *Trp53* expression was remarkably reduced in 4C11+ metastatic melanoma cells when compared to the melanocytes melan-a, non-tumorigenic 4C cells and tumorigenic 4C11- cells as analyzed by RT-PCR (**Figure 4A**). This result was confirmed by Western blotting analyses (**Figure 4B**) and immunofluorescence (**Figure 4C**), showing low levels of p53 protein in the metastatic melanoma lineage 4C11+.

Although the *TP53* mutations are relatively rare in human melanomas (0–17%), upstream pathways regulating p53 are frequently altered, as those involving ARF and MDM2 [3]. In our murine melanoma model, decreased *Trp53* expression in the metastatic 4C11+ melanoma cells are not associated with hotspot mutations clustered in the DNA-binding domain of *Trp53* gene, including exons 5, 6, 7 and 8, as evaluated by DNA sequencing (data not shown). A downregulation of p53 protein by its ubiquitination induced by MDM2 is unlikely since 4C11+ cells express neither *Trp53* mRNA (**Figure 4A**) nor p53 protein (**Figure 4B** and **C**). Moreover, treatment with the proteasome inhibitor MG132 does not result in increased level of p53 protein in the 4C11+ cells (**Figure S2**). On the other hand, by evaluating the level of p53 protein in the lineages derived from 4C11- cells, it was found that 4C11- miR-138 presents almost total loss of p53 protein levels compared to 4C11- and 4C11- mock (**Figure 4D**).

The 3'UTR is the canonical binding site for miRNAs, and it is through this miRNA-mRNA interaction that RISC complex proteins can promote degradation or prevent translation of mRNA targets. The analysis of *Trp53* 3'UTR revealed a single binding site for miR-138-5p (**Figure 4E**). To determine if *Trp53* is directly regulated by this miRNA, the 3'UTR of *Trp53* mRNA was cloned downstream of the firefly luciferase gene in the

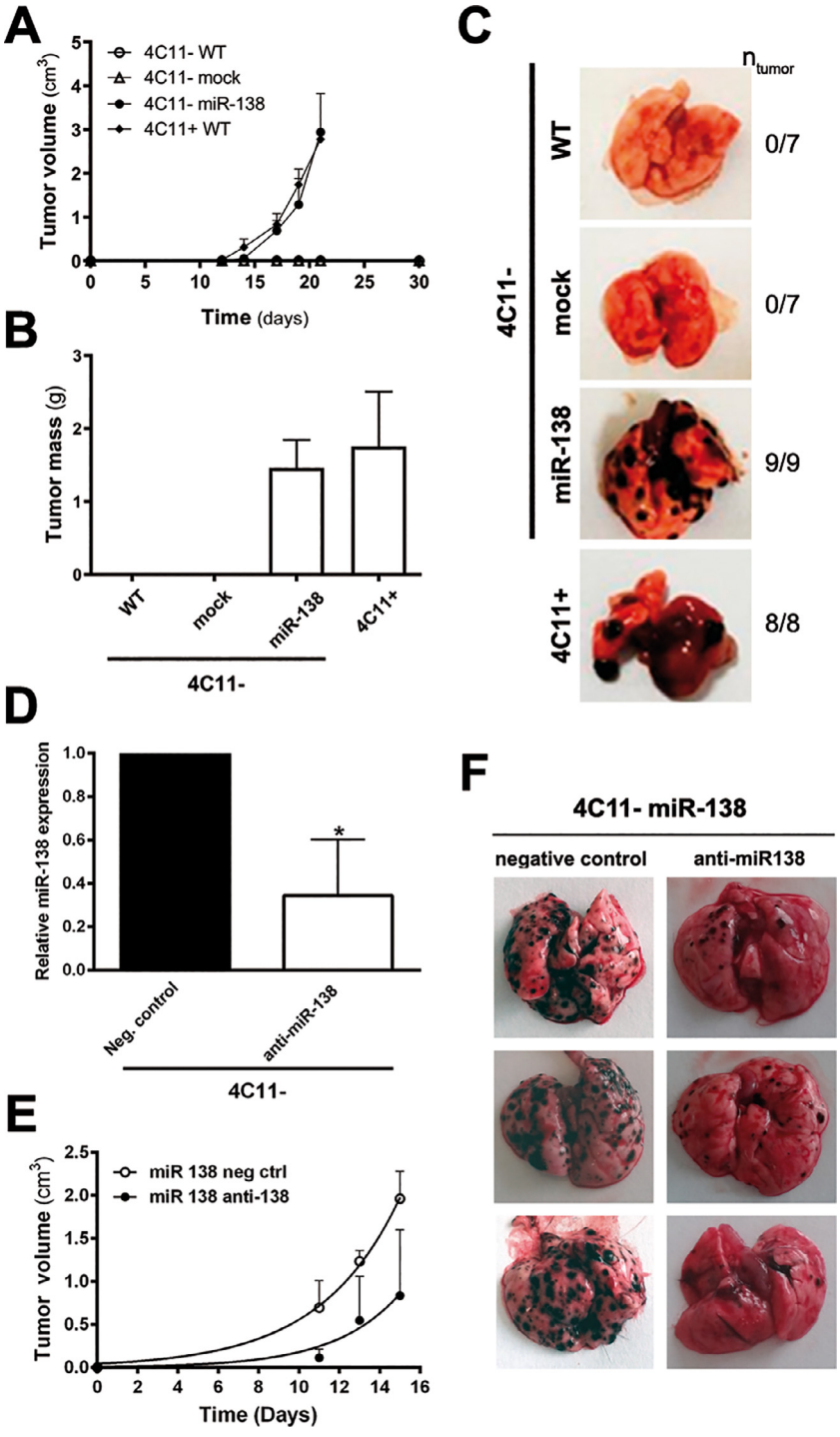

Fig. 3. Non-metastatic melanoma cells overexpressing miR-138-5p acquire metastatic traits. **A** and **B.** Tumor growth (**A**) and tumor mass (**B**) after s.c. injection of 2.5×10^5 cells in syngeneic mice. Tumor mass was measured at the end of the experiment (d 21). **C.** Metastatic capacity, revealed as colony formation in the lungs of syngeneic mice after i.v. (tail vein) injection of 2.5×10^5 cells. **D.** Expression of miR-138-5p in 4C11- miR-138 after antagomiR treatment. U6 expression was used as endogenous control for miR-138-5p expression. * $P < 0.01$. **E.** Tumor growth in syngeneic mice after s.c. injection of 2.5×10^5 4C11- miR-138 cells after antagomiR treatment. **F.** Metastatic capacity, represented by colonies in the lung after i.v. injection of 2.5×10^5 4C11- miR-138 cells after antagomiR treatment. 4C11- WT: non-metastatic melanoma cell line; 4C11- mock: 4C11- transduced with viruses containing an empty vector; 4C11- miR-138: 4C11- transduced with virus encoding the pre-miR138-5p and flanking sequences; and 4C11+: metastatic melanoma cell line. neg ctl: negative control.

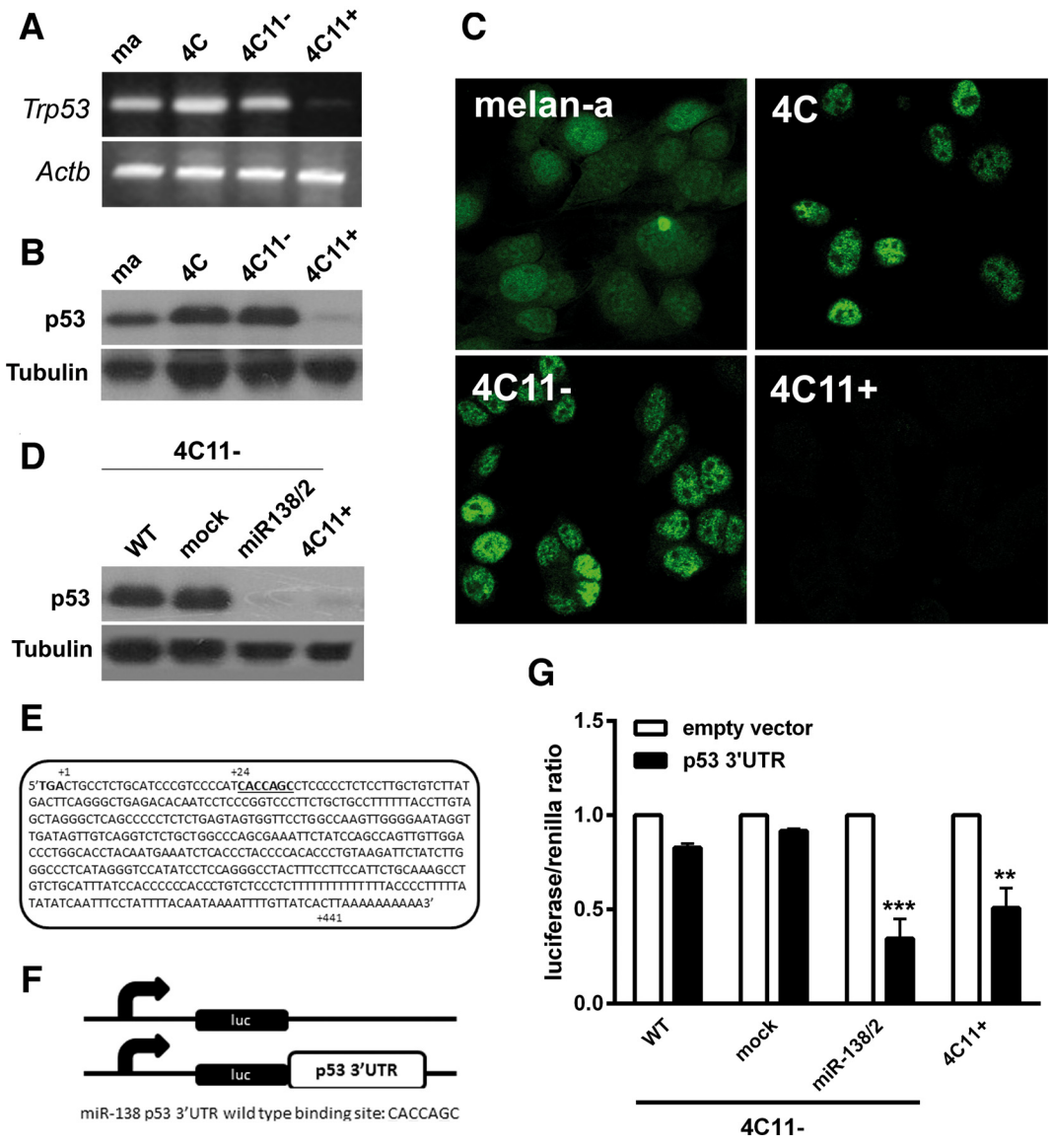

Fig. 4. *Trp53* is as a target of miR-138-5p in the metastatic 4C11+ cells. **A.** *Trp53* gene expression evaluated by RT-PCR in melan-a (ma), 4C, 4C11- and 4C11+ cell lines. p53 protein expression analyzed by Western blotting (**B**) and indirect immunofluorescence (**C**) in the cell lines that comprise the cellular murine model of melanoma progression. **D.** p53 protein expression in 4C11- cell line transduced with miR-138 or negative control as evaluated by Western blotting. **E.** The *Trp53* 3'UTR sequence presenting the binding site for miR-138-5p is highlighted. **F.** Construct used in the luciferase assay, in which the *Trp53* 3'UTR was inserted downstream of luciferase cDNA. **G.** Decreased luciferase activity indicates interaction between *Trp53* 3'UTR and miR-138-5p. ma: parental melan-a melanocytes; 4C: pre-malignant melanocytes; 4C11-: non-metastatic melanoma cell line; 4C11+: metastatic melanoma cell line; 4C11- WT: non-metastatic melanoma cell line; 4C11- mock: 4C11- transduced with viruses containing an empty vector; 4C11- miR-138: 4C11- transduced with virus containing the pre-miR138-5p and flanking sequences. ** $P < 0.001$, *** $P < 0.0001$.

pGL3control vector, generating the pGL3-p53 3'UTR construct (Figure 4**F**). The empty pGL3-control vector was used as a positive control of luciferase activity. As noted, the metastatic 4C11+, expressing high level of endogenous miR-138-5p, and the 4C11- miR-138 cells, with high amounts of exogenous miR-138-5p, when transfected with pGL3-p53 3'UTR, showed a decrease of 61% and 66% of luciferase firefly activity, respectively, compared to the cells lines transfected with the empty pGL3-control vector. 4C11- and 4C11- mock cell lines, which possess low levels of miR-138-5p expression, had a reduction of only 18% and 9%, respectively, of luciferase activity under the same conditions (Figure 4**G**).

High expression of hsa-miR-138-5p and low expression of p53 correlate with poor clinical outcomes of human melanoma patients

Finally, to transpose our findings from the murine model to human melanoma samples, we initially verified if miR-138-5p expression was altered in a set of 26 FFPE (Formalin-Fixed Paraffin-Embedded) samples: seven benign nevi, fourteen primary melanomas, and seven metastatic melanomas. Increased expression of hsa-miR-138-5p was observed in primary and metastatic melanomas compared to benign nevi (Figure 5**A**). Accessing public data sets of different melanoma cohorts, we found a

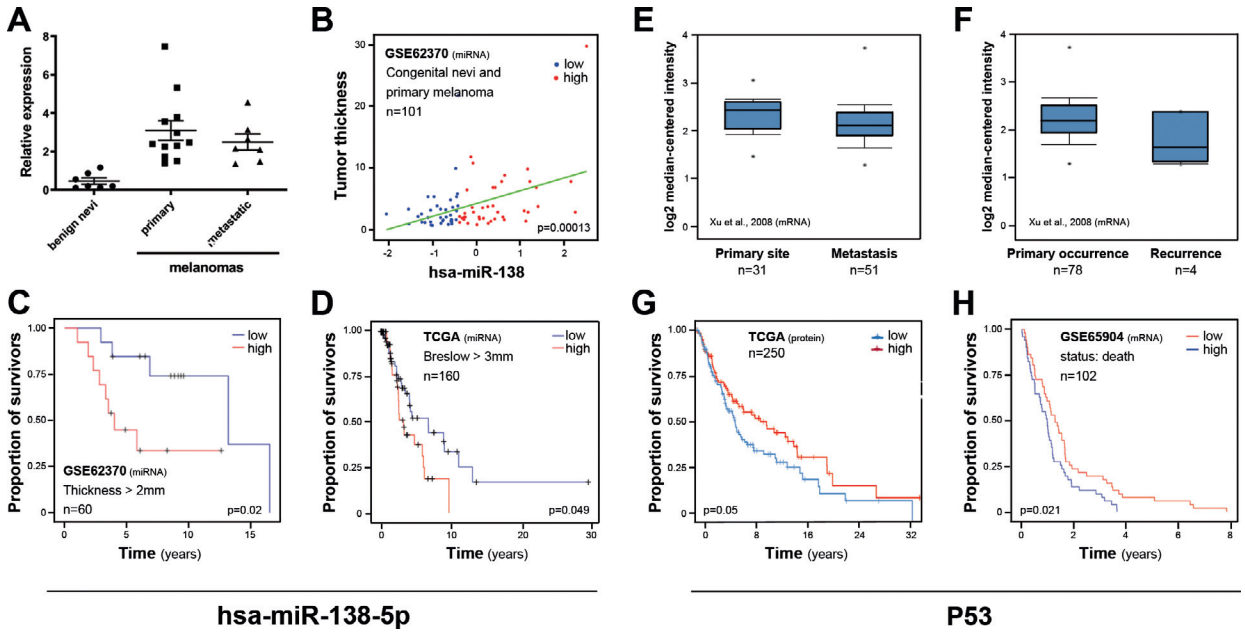

Fig. 5. High expression of miR-138-5p and low expression of p53 correlate with poor clinical outcomes of human melanoma patients. **A.** The expression of hsa-miR-138-5p was analyzed by real-time PCR in 7 benign *nevi*, 12 primary melanomas and 7 metastatic melanomas obtained from the Department of Pathology and Molecular Medicine from Kingston General Hospital, Kingston, Ontario, Canada. **B.** Significant correlation (slope = 2.06; $P = 0.00013$) between miR-138-5p expression and melanoma thickness in congenital nevi and primary melanoma samples (n = 101) (GSE62370). **C.** Primary melanoma tumors (GSE62370) with a thickness >2 (n = 60) that express high levels of miR-138-5p (25% upper quartile) have poor overall survival compared to those with low miRNA levels (25% lower quartile) ($P = 0.02$). **D.** Primary and metastatic melanomas (TCGA) with Breslow depth >3 mm (n = 160) have poor overall survival when expressing high levels (above median) of miR-138-5p compared to low levels (below median) ($P = 0.049$). **E.** Metastatic melanomas (n = 51) express lower levels of *TRP53* compared to primary melanomas (n = 31) (GSE8401). **F.** Recurrent melanomas (n = 4) express lower levels of *TP53* compared to melanomas of primary occurrence (n = 78) (GSE8401). **G.** Primary and metastatic melanomas (n = 250) (TCGA) expressing lower levels of p53 protein (below median) have poor overall survival compared to those expressing higher levels (above median) ($P = 0.05$). **H.** From patients who died from melanoma (n = 102), those expressing lower levels of *TP53* (below median) had poor overall survival compared with those with higher levels (above median) ($P = 0.021$) (primary and metastatic melanomas, GSE65904).

direct correlation between miR-138-5p expression and melanoma thickness (GSE62370, n = 101) (**Figure 5B**), poor overall survival for patients presenting melanomas with thickness greater than 2 mm and high miR-138-5p expression compared to those with low miRNA expression (GSE62370, n = 60) (**Figure 5C**), and poor overall survival for patients with melanomas with Breslow thickness greater than 3 mm and high miR-138-5p expression compared to those with low miRNa expression (TCGA, n = 160) (**Figure 5D**). Moreover, in a study published by Xu and colleagues [52]; GSE8401), lower levels of *TP53* were observed in metastatic compared to primary melanomas (**Figure 5E**), and in those melanoma samples from recurrence compared to primary occurrence (**Figure 5F**). In a different cohort, patients bearing melanomas with lower p53 protein levels had poor overall survival compared to those with higher levels (TCGA, n = 250) (**Figure 5G**). In addition, for patients who died from melanoma, the lower *TP53* expression also correlated with poor overall survival (TCGA, n = 102) (**Figure 5H**).

Discussion

miR-138-5p is recognized as an important molecule in the development of the nervous system and also in maintaining its homeostasis. In fact, the first discovery regarding the miR-138 sequence was made in nervous system tissues [15], where it contributes to the migration of hypothalamic neurons [16] - cells with the same embryonic origin as melanocytes. In the present work, we provide evidence that miR-138-5p is involved in the progression of melanoma to a metastatic state through the regulation of P53. Increased expression of miR-138-5p was found in 4C11+ metastatic melanoma cells compared to non-metastatic melanoma cells (**Figure 1B**), suggesting its participation in the acquisition of an aggressive phenotype. Indeed, increased miR-138-5p expression in human metastatic melanoma was observed by several independent groups analyzing the expression of miRNA sets [2,6,12,37,38], suggesting its involvement in human melanoma progression. To further investigate this miRNA involvement with melanoma aggressiveness, the non-metastatic melanoma 4C11- cell line, which express low endogenous levels of miR-138-5p, was handled to overexpress miR-138-5p (**Figure 1**, **C** and **D**). miR-138-5p overexpression was associated with the increase of 4C11- miR-138 cell proliferation (**Figure 2**, **B** and **D**) and clonogenic capability (**Figure 2E**). The contribution of miR-138-5p in cell survival was previously described in glioma pluripotent cells (GSCs) and gastric cancer cells. miR-138 inhibition reduced GSCs proliferation, survival and colony formation, indicating its participation as an oncogene in glioma carcinogenesis [6]. Increased miR-138-5p expression also renders 4C11- miR-138 more resistant to *anoikis* (**Figure 2C**), what is in agreement with its role in triple-negative breast cancer cells in abrogating apoptosis by targeting TUSC2, a pro-apoptotic tumor suppressor gene [31]. Collective migration capacity was also augmented by miR-138-5p overexpression (**Figure 2F**), suggesting its participation in metastasis. Corroborating with the role of miR-138-5p in melanoma migration, miR-138-5p overexpression induced the reorganization of the actin cytoskeletal leading to the formation of lamellipodia, membrane projections on the leading edge of migratory cells. Increased FAK phosphorylation on the migration front was also observed. FAK phosphorylation is associated with spreading process and

turnover of focal contacts, leading to cell migration [47]. The importance of phosphorylated FAK in cell migration and metastasis has been demonstrated since FAK phosphorylation inhibition was shown to decrease metastatic capability in breast cancer and lung cancer cells [21,40]. miR-138 is also related to migration of hypothalamic neurons via direct regulation of Reelin [16], a glycoprotein that plays a critical role in neuronal migration during brain development [9]. These data suggest that miR-138 has influence over migration of cells of nervous origin. The 4C11- miR-138 cells also developed fast-growing tumors and acquired metastatic capacity, as evidenced by *in vivo* experiments (**Figure 3C**). Moreover, inhibition of miR-138-5p by its antagomiR in 4C11- miR-138 caused a significant reduction in metastatic *foci* in lungs (**Figure 3F**). Next-generation sequencing of small RNAs isolated from a series of annotated melanomas revealed a set of top 40 list that were differentially expressed between thin and thick melanomas, correlating with clinical and melanoma American Joint Committee on Cancer (AJCC) prognostic parameters, including Breslow's depth invasion [2]. Among others, miR-138-5p was found to be overexpressed in thick melanomas when compared with thin melanomas, suggesting that its expression correlates with disease severity. Increased miR138-5p expression in nodular melanoma when compared to superficial spreading melanoma also supported its participation in the acquisition of an invasive and aggressive melanoma phenotype [38]. While some groups have reported decreased miR-138 expression during tumor progression and consider it a potential tumor suppressor molecule [22,26,56], while we and others observed that miR-138 promotes the acquisition of malignant characteristics and can act as an oncogene [24,50]. Very recently, [30] identified that miR-138-5p is involved with aggressive clinicopathological features. By analyzing a series of 179 FFPE primary cutaneous melanomas, they found a significant correlation between high expression of miR-138-5p and greater Breslow thickness, ulceration, and mitosis.

We verified that overexpression of miR-138 contributes to modifications in 4C11- cells as seen by the gain in migratory and proliferative capacity, the ability to survive in conditions of stress (represented by the absence of FBS in the culture medium) and anchorage blockade. The search for a miR-138 target that could explain these changes pointed to *Trp53* as a strong candidate. First, *Trp53* was described as a putative target of miR-138 using several prediction sites. Although *Trp53* is frequently mutated in many tumors, mutations in *Trp53* are relatively rare in melanomas [23,25,49] with wild-type P53 protein typically expressed despite the fact that this tumor type is particularly radioresistant (Bradbury et al., 1994); [14]. Following, mutational analysis of the *Trp53* gene hot spots by DNA sequencing in the cell lines melan-a, 4C, 4C11- and 4C11+ showed no mutations (data not shown). Interestingly, decreased *TP53* gene expression (**Figure 4A**) and protein amount (**Figure 4**, **B** and **C**) was only observed in 4C11+ metastatic melanoma cells when compared with 4C11- non-metastatic melanoma cells, reinforcing its role in the acquisition of an aggressive phenotype. There are several mechanisms by which wild-type p53 function can be inhibited in melanoma, as high levels of MDM2 or the disruption of signaling pathways that activate p53 in response to DNA damage [41]. However, treatment of 4C11+ melanoma cells with a proteasome inhibitor did not increase p53 expression (**Figure S2**). Imbalance of miRNAs that target *Trp53* can also explain the differential expression of p53 detected throughout human melanoma development. Recent studies have shown that p53 metastasis regulation is mediated by miRNA-dependent mechanisms, decreasing the expression of master regulators of epithelial-to-mesenchymal transition (EMT), such as TWIST1 and SNAIL, which in turn, abrogate EMT, the acquisition of stem cell-like properties and migration of breast cancer cells [7,53]. Moreover, it has been shown that pluripotent stem cell induction is mediated by miR-138-5p through regulation of p53 signaling pathway [54]. P53 regulation by miR-138-5p was also demonstrated in liver macrophages [51]. In our model, overexpression of miR-138-5p in 4C11- melanoma cells reduced p53 protein (**Figure 4D**), suggesting that p53 expression is regulated by miR-138-5p in melanoma. In addition, sequencing of the *Trp53* 3′UTR region, which contains a miR-138-5p binding site, in the metastatic melanoma strain 4C11+, revealed no mutations confirming that the miRNA binding region is intact. To determine whether the *Trp53* is a direct target of miR-138-5p, a reporter gene assay was performed. Cells with elevated expression of miR-138-5p (4C11- miR-138 and lineage 4C11+) presented reduced luciferase activity when transfected with *Trp53* 3'UTR containing strains (**Figure 4G**). The luciferase assay in combination with the sequencing data confirmed that *Trp53* is a direct target of miR-138-5p.

Using data sets of independent melanoma cohorts (TCGA, GSE62370, GSE65904, and GSE8401), we found a prognostic value of miR-138-5p and *TP53*/p53 in the clinical outcome of melanoma patients. Together, these findings highlight the potential predictive clinical value of mir-138-5p and its role in regulating p53 expression and conferring aggressive traits to melanoma cells.

Conclusions

The findings of the present work reveal that miR-138-5p contributes to melanoma progression. Moreover, the acquisition of an aggressive cellular phenotype due to overexpression of miR-138-5p may be explained, at least in part, by the reduction of p53 protein expression.

Consent for publication

Not applicable.

Ethics approval and consent to participate

All animal procedures used in this study were approved by the Ethics Committee from Universidade Federal de São Paulo (number 2118/11). The study with the human melanocytic lesions from paraffin embedded tissues obtained from the Department of Pathology and Molecular Medicine of the Kingston General Hospital was approved by the Ethics Committee from Health Sciences College at Queen's University.

Availability of data and material

All data generated and/or analyzed during this study are included in this published article. Some additional information can be requested for the authors.

Author contributions

Conceived and designed the experiments: ATC, MGJ. Performed the experiments: ATC, AH, ACM, ALPA, GCP, DL, EMC, FHMM. Analyzed the data: ATC, MGJ. Contributed reagents/materials/analysis: ATC, JFSF, BES, VT, RSS, MGJ. Wrote the paper: ATC, FHMM, DKA, ALPA, MGJ. All authors read and approved the final manuscript. ATC: Conceptualization, Methodology, Investigation, Writing - Original Draft, Visualization; AH: Methodology; FHMM: Investigation, Writing - Original Draft; ACM: Methodology, Formal analysis, Data Curation; GCP: Methodology; DL: Methodology; DKAF: Validation, Investigation, Writing - Review & Editing; ALPA: Validation, Investigation, Writing - Review & Editing; Esteban Mauricio Cordero: Methodology, Writing - Review & Editing; José Franco da Silveira Filho: Methodology, Writing - Review & Editing; Regine Schneider-Stock: Methodology, Resources, Writing - Review & Editing; Bryan Eric Strauss: Methodology, Writing - Review & Editing; Victor Tron: Methodology, Resources, Supervision; MGJ: Conceptualization, Methodology, Resources, Writing - Review & Editing, Visualization, Supervision, Project administration, Funding acquisition.

Supplementary materials

Supplementary material associated with this article can be found, in the online version, at doi:10.1016/j.neo.2021.05.015.

References

[1] Agarwal V, Bell GW, Nam J, Bartel DP. Predicting effective microRNA target sites in mammalian mRNAs. *eLife* 2015;**4**:e05005. doi:10.7554/eLife.05005.

[2] Babapoor S, Wu R, Kozubek J, Auidi D, Grant-Kels JM, Dadras SS. Identification of microRNAs associated with invasive and aggressive phenotype in cutaneous melanoma by next-generation sequencing. *Lab. Invest* 2017;**97**(6):636–48. doi:10.1038/labinvest.2017.5.

[3] Basu S, Murphy ME. Genetic modifiers of the p53 pathway. *Cold Spring Harb. Perspect. Med* 2016;**6**(4):a026302. doi:10.1101/cshperspect.a026302.

[4] Bennett DC, Cooper PJ, Hart IR. A line of non-tumorigenic mouse melanocytes, syngeneic with the B16 melanoma and requiring a tumour promoter for growth. *Int. J. Cancer* 1987;**39**(3):414–18. doi:10.1002/ijc.2910390324.

[5] Caramuta S, Egyházi S, Rodolfo M, Witten D, Hansson J, Larsson C, Lui WO. MicroRNA expression profiles associated with mutational status and survival in malignant melanoma. *J Invest Dermatol* 2010;**130**(8):2062–70. doi:10.1038/jid.2010.63.

[6] Chan XHD, Nama S, Gopal F, Rizk P, Ramasamy S, Sundaram G, Ow GS, Ivshina AV, Tanavde V, Haybaeck J, et al. Targeting glioma stem cells by functional inhibition of a prosurvival oncomiR-138 in malignant gliomas. *Cell Rep* 2012;**2**(3):591–602. doi:10.1016/j.celrep.2012.07.012.

[7] Chang CJ, Chao CH, Xia W, Yang JY, Xiong Y, Li CW, Yu WH, Rehman SK, Hsu JL, Lee HH, et al. p53 regulates epithelial-mesenchymal transition and stem cell properties through modulating miRNAs. *Nat Cell Biol* 2011;**13**(3):317–23. doi:10.1038/ncb2173.

[8] Chen J, Feilotter HE, Paré GC, Zhang X, Pemberton JG, Garady C, Lai D, Yang X, Tron VA. MicroRNA-193b represses cell proliferation and regulates cyclin D1 in melanoma. *Am J Pathol* 2010;**176**(5):2520–9. doi:10.2353/ajpath.2010.091061.

[9] Dohi O, Takada H, Wakabayashi N, Yasui K, Sakakura C, Mitsufuji S, Naito Y, Taniwaki M, Yoshikawa T. Epigenetic silencing of RELN in gastric cancer. *Int J Oncol* 2010;**36**(1):85–92.

[10] Ghatak D, Das Ghosh D, Roychoudhury S. Cancer Stemness: p53 at the Wheel. *Front Oncol* 2021;**10**:604124. doi:10.3389/fonc.2020.604124.

[11] Gaur A, Jewell DA, Liang Y, Ridzon D, Moore JH, Chen C, Ambros VR, Israel MA. Characterization of microRNA expression levels and their biological correlates in human cancer cell lines. *Cancer Res* 2007;**67**(6):2456–68. doi:10.1158/0008-5472.CAN-06-2698.

[12] Greenberg E, Hershkovitz L, Itzhaki O, Hajdu S, Nemlich Y, Ortenberg R, Gefen N, Edry L, Modai S, Keisari Y, et al. Regulation of cancer aggressive features in melanoma cells by microRNAs. *PLoS One* 2011;**6**(4):e18936. doi:10.1371/journal.pone.0018936.

[13] Hodis E, Watson IR, Kryukov GV, Arold ST, Imielinski M, Theurillat JP, Nickerson E, Auclair D, Li L, Place C, et al. A landscape of driver mutations in melanoma. *Cell* 2012;**150**(2):251–63. doi:10.1016/j.cell.2012.06.024.

[14] Jenrette JM. Malignant melanoma: the role of radiation therapy revisited. *Semin Oncol* 1996;**23**(6):759–62.

[15] Kim J, Krichevsky A, Grad Y, Hayes GD, Kosik KS, Church GM, Ruvkun G. Identification of many microRNAs that copurify with polyribosomes in mammalian neurons. *Proc Natl Acad Sci USA* 2004;**101**(1):360–5. doi:10.1073/pnas.2333854100.

[16] Kisliouk T, Meiri N. MiR-138 promotes the migration of cultured chicken embryonic hypothalamic cells by targeting reelin. *Neuroscience* 2013;**238**:114–24. doi:10.1016/j.neuroscience.2013.02.020.

[17] Kozubek J, Ma Z, Fleming E, Duggan T, Wu R, Shin DG, Dadras SS. In-depth characterization of microRNA transcriptome in melanoma. *PLoS One* 2013;**8**(9):e72699. doi:10.1371/journal.pone.0072699.

[18] Lankenau MA, Patel R, Liyanarachchi S, Maharry SE, Hoag KW, Duggan M, Walker CJ, Markowitz J, Carson WE 3rd, Eisfeld AK, et al. MicroRNA-3151 inactivates TP53 in BRAF-mutated human malignancies. *Proc Natl Acad Sci USA* 2015;**112**(49):E6744–51. doi:10.1073/pnas.1520390112.

[19] Li J, Akbani R, Zhao W, Lu Y, Weinstein JN, Gordon BM, Liang H. Explore, Visualize, and Analyze Functional Cancer Proteomic Data Using the Cancer Proteome Atlas. *Cancer Res* 2017;**77**(21):e51–4. doi:10.1158/0008-5472.CAN-17-0369.

[20] Li J, Lu Y, Akbani R, Ju Z, Roebuck PL, Liu W, Yang JY, Broom B, Verhaak R, Kane D, et al. TCPA: a resource for cancer functional proteomics data. *Nat Methods* 2013;**10**(11):1046–7. doi:10.1038/nmeth.2650.

[21] Liu W, Liang Y, Chan Q, Jiang L, Dong J. CX3CL1 promotes lung cancer cell migration and invasion via the Src/focal adhesion kinase signaling pathway. *Oncol Rep* 2019;**41**(3):1911–17. doi:10.3892/or.2019.6957.

[22] Liu X, Jiang L, Wang A, Yu J, Shi F, Zhou X. MicroRNA-138 suppresses invasion and promotes apoptosis in head and neck squamous cell carcinoma cell lines. *Cancer Lett* 2009;**286**(2):217–22. doi:10.1016/j.canlet.2009.05.030.

[23] Lubbe J, Reichel M, Burg G, Kleihues P. Absence of p53 gene mutations in cutaneous melanoma. *J Invest Dermatol* 1994;**102**(5):819–21. doi:10.1111/1523-1747.ep12381544.

[24] Luo D, Wilson JM, Harvel N, Liu J, Pei L, Huang S, Hawthorn L, Shi H. A systematic evaluation of miRNA:mRNA interactions involved in the migration and invasion of breast cancer cells. *J Transl Med* 2013;**11**:57. doi:10.1186/1479-5876-11-57.

[25] Miller AJ, Mihm MC, Melanoma Jr. *N Engl J Med* 2006;**355**(1):51–65. doi:10.1056/NEJMra052166.

[26] Mitomo S, Maesawa C, Ogasawara S, Iwaya T, Shibazaki M, Yashima-Abo A, Kotani K, Oikawa H, Sakurai E, Izutsu N, et al. Downregulation of miR-138 is associated with overexpression of human telomerase reverse transcriptase protein in human anaplastic thyroid carcinoma cell lines. *Cancer Sci* 2008;**99**(2):280–6. doi:10.1111/j.1349-7006.2007.00666.x.

[27] Molognoni F, Cruz AT, Meliso FM, Morais AS, Souza CF, Xander P, Bischof JM, Costa FF, Soares MB, Liang G, et al. Epigenetic reprogramming as a key contributor to melanocyte malignant transformation. *Epigenetics* 2011;**6**(4):450–64. doi:10.4161/epi.6.4.14917.

[28] Mozūraitienė J, Bielskienė K, Atkočius V, Labeikytė D. Molecular alterations in signal pathways of melanoma and new personalized treatment strategies: Targeting of Notch. Medicina *(Kaunas)* 2015;**51**(3):133–45. doi:10.1016/j.medici.2015.06.002.

[29] Mueller DW, Rehli M, Bosserhoff AK. miRNA expression profiling in melanocytes and melanoma cell lines reveals miRNAs associated with formation and progression of malignant melanoma. *J Invest Dermatol* 2009;**129**(7):1740–51. doi:10.1038/jid.2008.452.

[30] Murria Estal R, de Unamuno Bustos B, Pérez Simó G, Simarro Farinos J, Torres Navarro I, Alegre de Miquel V, Ballester Sánchez R, Sabater Marco V, Llavador Ros M, Palanca Suela S, et al. MicroRNAs expression associated with aggressive clinicopathological features and poor prognosis in primary cutaneous melanomas. *Melanoma Res* 2021;**31**(1):18–26. doi:10.1097/CMR.0000000000000709.

[31] Nama S, Muhuri M, Di Pascale F, Quah S, Aswad L, Fullwood M, Sampath P. MicroRNA-138 is a Prognostic Biomarker for Triple-Negative Breast Cancer and Promotes Tumorigenesis via TUSC2 repression. *Sci Rep* 2019;**9**(1):12718. doi:10.1038/s41598-019-49155-4.

[32] Oba-Shinjo SM, Correa M, Ricca TI, Molognoni F, Pinhal MA, Neves IA, Marie SK, Sampaio LO, Nader HB, Chammas R, et al. Melanocyte transformation associated with substrate adhesion impediment. *Neoplasia* 2006;**8**(3):231–41. doi:10.1593/neo.05781.

[33] Obernosterer G, Leuschner PJ, Alenius M, Martinez J. Post-transcriptional regulation of microRNA expression. *RNA* 2006;**12**(7):1161–7. doi:10.1261/rna.232250.

[34] Parfenyev S, Singh A, Fedorova O, Daks A, Kulshreshtha R, Barlev NA. Interplay between p53 and non-coding RNAs in the regulation of EMT in breast cancer. *Cell Death Dis* 2021;**12**(1):17. doi:10.1038/s41419-020-03327-7.

[35] Park D, Kim H, Kim Y, Jeoung D. miR-30a regulates the expression of CAGE and p53 and regulates the response to anti-cancer drugs. *Mol Cells* 2016;**39**(4):299–309. doi:10.14348/molcells.2016.2242.

[36] Patton EE, Widlund HR, Kutok JL, Kopani KR, Amatruda JF, Murphey RD, Berghmans S, Mayhall EA, Traver D, Fletcher CD, et al. BRAF mutations are sufficient to promote nevi formation and cooperate with p53 in the genesis of melanoma. *Curr Biol* 2005;**15**(3):249–54. doi:10.1016/j.cub.2005.01.031.

[37] Philippidou D, Schmitt M, Moser D, Margue C, Nazarov PV, Muller A, Vallar L, Nashan D, Behrmann I, Kreis S. Signatures of microRNAs and selected microRNA target genes in human melanoma. *Cancer Res* 2010;**70**(10):4163–73. doi:10.1158/0008-5472.CAN-09-4512.

[38] Poliseno L, Haimovic A, Segura MF, Hanniford D, Christos PJ, Darvishian F, Wang J, Shapiro RL, Pavlick AC, Berman RS, et al. Histology-specific microRNA alterations in melanoma. *J Invest Dermatol* 2012;**132**(7):1860–8. doi:10.1038/jid.2011.451.

[39] Rhodes DR, Yu J, Shanker K, Deshpande N, Varambally R, Ghosh D, Barrette T, Pandey A, Chinnaiyan AM. ONCOMINE: a cancer microarray database and integrated data-mining platform. *Neoplasia* 2004;**6**(1):1–6. doi:10.1016/s1476-5586(04)80047-2.

[40] Rigiracciolo DC, Santolla MF, Lappano R, Vivacqua A, Cirillo F, Galli GR, Talia M, Muglia L, Pellegrino M, Nohata N, et al. Focal adhesion kinase (FAK) activation by estrogens involves GPER in triple-negative breast cancer cells. *J Exp Clin Cancer Res* 2019;**38**(1):58. doi:10.1186/s13046-019-1056-8.

[41] Satyamoorthy K, Chehab NH, Waterman MJ, Lien MC, El-Deiry WS, Herlyn M, Halazonetis TD. Aberrant regulation and function of wild-type p53 in radioresistant melanoma cells. *Cell Growth Differ* 2000;**11**(9):467–74.

[42] Sha HH, Wang DD, Chen D, Liu SW, Wang Z, Yan DL, Dong SC, Feng JF. MiR-138: A promising therapeutic target for cancer. *Tumor Biol* 2017;**39**(4):1–10. doi:10.1177/1010428317697575.

[43] Shain AH, Joseph NM, Yu R, Benhamida J, Liu S, Prow T, Ruben B, North J, Pincus L, Yeh I, et al. Genomic and transcriptomic analysis reveals incremental disruption of key signaling pathways during melanoma evolution. *Cancer Cell* 2018;**34**(1):45–55 .e4. doi:10.1016/j.ccell.2018.06.005.

[44] Slack FJ, Chinnaiyan AM. The Role of Non-coding RNAs in Oncology. *Cell* 2019;**179**(5):1033–55. doi:10.1016/j.cell.2019.

[45] Souza CF, Xander P, Monteiro AC, Silva AG, da Silva DC, Mai S, Bernardo V, Lopes JD, Jasiulionis MG. Mining gene expression signature for the detection of pre-malignant melanocytes and early melanomas with risk for metastasis. *PLoS One* 2012;**7**(9):e44800. doi:10.1371/journal.pone.0044800.

[46] Strbenac D, Wang K, Wang X, Dong J, Mann GJ, Mueller S, Yang JYH. Melanoma Explorer: a web application to allow easy reanalysis of publicly available and clinically annotated melanoma omics data sets. *Melanoma Res* 2019;**29**(3):342–4. doi:10.1097/CMR.0000000000000533.

[47] Tapial Martínez P, López Navajas P, Lietha D. FAK structure and regulation by membrane interactions and force in focal adhesions. *Biomolecules* 2020;**10**(2):179. doi:10.3390/biom10020179.

[48] The Cancer Genome Atlas NetworkGenomic classification of cutaneous melanoma. *Cell* 2015;**161**(7):1681–96. doi:10.1016/j.cell.2015.05.044.

[49] Volkenandt M, Schlegel U, Nanus DM, Albino AP. Mutational analysis of the human p53 gene in malignant melanoma. *Pigment Cell Res* 1991;**4**(1):35–40. doi:10.1111/j.1600-0749.1991.tb00311.x.

[50] Wang Y, Huang JW, Li M, Cavenee WK, Mitchell PS, Zhou X, Tewari M, Furnari FB, Taniguchi T. MicroRNA-138 modulates DNA damage response by repressing histone H2AX expression. *Mol Cancer Res* 2011;**9**(8):1100–11. doi:10.1158/1541-7786.MCR-11-0007.

[51] Wang YQ, Lan YY, Guo YC, Yuan QW, Liu P. Down-regulation of microRNA-138 improves immunologic function via negatively targeting p53 by regulating liver macrophage in mice with acute liver failure. *Biosci. Rep.* 2019;**39**(7):BSR20190763. doi:10.1042/BSR20190763.

[52] Xu L, Shen SS, Hoshida Y, Subramanian A, Ross K, Brunet JP, Wagner SN, Ramaswamy S, Mesirov JP, Hynes RO. Gene expression changes in an animal melanoma model correlate with aggressiveness of human melanoma metastases. *Mol Cancer Res* 2008;**6**(5):760–9. doi:10.1158/1541-7786.MCR-07-0344.

[53] Yang-Hartwich Y, Tedja R, Roberts CM, Goodner-Bingham J, Cardenas C, Gurea M, Sumi NJ, Alvero AB, Glackin CA, Mor G. p53-pirh2 complex promotes twist1 degradation and inhibits EMT. *Mol Cancer Res* 2019;**17**(1):153–64. doi:10.1158/1541-7786.MCR-18-0238.

[54] Ye D, Wang G, Liu Y, Huang W, Wu M, Zhu S, Jia W, Deng AM, Liu H, Kang J. MiR-138 promotes induced pluripotent stem cell generation through the regulation of the p53 signaling. *Stem Cells* 2012;**30**(8):1645–54. doi:10.1002/stem.1149.

[55] Yu H, McDaid R, Lee J, Possik P, Li L, Kumar SM, Elder DE, Van Belle P, Gimotty P, Guerra M, et al. The role of BRAF mutation and p53 inactivation during transformation of a subpopulation of primary human melanocytes. *Am J Pathol* 2009;**174**(6):2367–77. doi:10.2353/ajpath.2009.081057.

[56] Zhao X, Yang L, Hu J, Ruan J. miR-138 might reverse multidrug resistance of leukemia cells. *Leuk Res* 2010;**34**(8):1078–82. doi:10.1016/j.leukres.2009.10.002.